Continental Shelf Research 132 (2017) 29–37

Contents lists available at ScienceDirect

Continental Shelf Research

journal homepage: www.elsevier.com/locate/csr

Research papers

Distribution and mass inventory of mercury in sediment from the Yangtze River estuarine-inner shelf of the East China Sea

Wenchuan Liu[a], Limin Hu[b,c,*], Tian Lin[d], Yuanyuan Li[a], Zhigang Guo[a,**]

[a] Shanghai Key Laboratory of Atmospheric Particle Pollution Prevention, Department of Environmental Science and Engineering, Fudan University, Shanghai 200433, China
[b] Key Laboratory of Marine Sedimentology and Environmental Geology, First Institute of Oceanography, State Oceanic Administration, Qingdao 266061, China
[c] Laboratory for Marine Geology, Qingdao National Laboratory for Marine Science and Technology, Qingdao 266061, China
[d] State Key Laboratory of Environmental Geochemistry, Institute of Geochemistry, Chinese Academy of Sciences, Guiyang 550081, China

ARTICLE INFO

Keywords:
Mercury
Surface sediments
Distribution
Mass inventory
Large river input
The coastal East China Sea

ABSTRACT

Mercury (Hg) was measured in 70 sediment samples from the Yangtze River estuarine-inner shelf of the East China Sea (ECS) to evaluate its occurrence, distribution, and deposition flux. Its concentrations were 10–92 ng/g with a mean of 46 ± 17 ng/g. A decrease of Hg concentration with increasing distance offshore suggested a dominance of riverine input. The high levels of Hg observed at the southern inner shelf were partly due to the sorption affinity of fine-grained sediments. Hg concentration was significantly correlated with total organic carbon content and sediment grain size, implying that the nature of sedimentary organic matter and hydrodynamic forces could influence the Hg occurrence. A moderate correlation between Hg with high-molecular-weight polycyclic aromatic hydrocarbons in the YRE suggested that they shared a similar input pathway. The total deposition flux of Hg was estimated to be ~52 t/y with a deposition rate of 6–120 ng/cm^2 y, which indicated that the estuarine-inner shelf of the ECS was a major sink of Hg in the margins off China, and this area could play a significant role in the Hg biogeochemical cycle on a global scale.

1. Introduction

Mercury (Hg) is a highly toxic element that can adversely affect organisms; however, its toxicity depends mainly on its chemical form (Li et al., 2011). Approximately 95% of atmospheric Hg occurs as gaseous elemental Hg^0 (Schroeder and Munthe, 1998), which has a long atmospheric residence time and can be transported globally due to its low reactivity and stability. The high vapor pressure and low oxidation potential make it uneasy to be scavenged and deposited via wet or dry deposition before oxidation to Hg^{2+}(Hylander and Goodsite, 2006; Lindberg et al., 2007). Elemental Hg can be released into the environment from natural and anthropogenic sources (Gustin et al., 2008). Global Hg emissions are dominated by anthropogenic sources, particularly the combustion of coal and petroleum products (Streets et al., 2005; Keeler et al., 2006; Lindberg et al., 2007).

In aquatic systems, sediments are usually considered as an ultimate sink of pollutants discharged from land-based sources, such as heavy metals and persistent organic pollutants either by atmospheric deposition or riverine input (Frignani et al., 2005; Elbaz-Poulichet et al., 2011; Li et al., 2012; Hu et al., 2014). Mercury can be accumulated in sediments and be released to surrounding media (Stein et al., 1996). It has potential toxic effects on biological resources, and indirectly, on human health (Peng et al., 2009; Chakraborty et al., 2010; Ernst, 2012; Pena-Fernandez et al., 2014).

Once Hg^0 is released into the air, it undergoes a series of complex transportation and transformation processes. In the presence of atomic bromine or ozone and hydrogen, Hg^0 can be oxidized to Hg^{2+}(Holmes et al., 2006). The resulting Hg^{2+} is deposited onto land and water, which can be absorbed by inorganic particles, biological particles, or organic matter (OM) (Ullrich et al., 2001). Inorganic Hg can be converted into organic Hg via biomethylation or abiotic methylation, and because organic forms of Hg, such as methylmercury, can be decomposed by solar ultraviolet radiation, methylation reactions are poor in water; therefore, sediments are considered as the main production site of methylmercury (Jonsson et al., 2012; Moreno et al., 2013; Zhang et al., 2014).

** Corresponding author.
* Corresponding author at: Key Laboratory of Marine Sedimentology and Environmental Geology, First Institute of Oceanography, State Oceanic Administration, Qingdao 266061, China.
E-mail addresses: hulimin@fio.org.cn (L. Hu), guozgg@fudan.edu.cn (Z. Guo).

http://dx.doi.org/10.1016/j.csr.2016.11.004
Received 4 December 2015; Received in revised form 6 November 2016; Accepted 10 November 2016
Available online 17 November 2016

The coast of the East China Sea (ECS) is one of the most developed regions in China, providing 42% of China's gross domestic product and housing 400 million inhabitants (Yang et al., 2006; Li et al., 2015). The origins of Hg in the regional-scale could be mainly derived from coal combustion and various industrial emissions; and recent rapid economic development and industrialization in this region has resulted in significant deposition of anthropogenic heavy metals, including Hg, into the coastal ECS from the Yangtze River (Streets et al., 2005; Lindberg et al., 2007; Chen et al., 2014; Wang et al., 2014, 2015). As the fifth largest river in water discharge and the fourth largest one in sediment discharge in the world, the Yangtze River has its drainage basin of ~1.94×10^6 km^2, which accounts for about 20% of the area of Mainland China (Yang et al., 2006; Bianchi and Allison, 2009). Discharged sediments and associated pollutants are primarily trapped in the Yangtze River Estuary (YRE) and the inner shelf of the ECS due to the net effects of the shear forces of coastal currents (Milliman et al., 1985; Liu et al., 2006, 2007; Bianchi and Allison, 2009; Li et al., 2012).

The distribution and input of Hg into the coastal margin have been recently explored around the world, for examples, Amos et al. (2014) reported the global biogeochemical implications of Hg discharges from rivers and sediment burial, and indicated that the burial of Hg in ocean margin sediments represents a major sink in the global Hg biogeochemical cycle. Liu et al. (2016) simulated and calculated Hg export from mainland China to adjacent seas. There have been some efforts to study Hg contamination in the sediments from several estuaries and coastal regions in coastal China seas, including the Bohai Sea (Luo et al., 2010), the ECS (Fang and Chen, 2010; Meng et al., 2014), the Xiamen Bay (Yan et al., 2010), the Pearl River Estuary, and the coastal region of Hong Kong (Zhou et al., 2007). However, there has been no systematic study found on the distribution and mass inventory of Hg in sediments of the inner shelf in the ECS, and the literature is particularly lacking in source-to-sink processes and the fate of Hg in the river-dominated coastal margin. The estuarine-inner shelf region of the ECS is a typical alongshore sediment dispersal system due to the large river discharge and sedimentary dynamics and thus can serve as an ideal natural experiment area for the study of deposition and fate of anthropogenic pollutants. In this study, we examined the concentration, distribution and inventory of Hg in sediments of the estuarine-inner shelf of the ECS, and identified potential factors influencing the source-to-sink processes of Hg in this region.

2. Materials and methods

2.1. Sampling

In total, the selected 70 surface sediment samples (0–3 cm) from the Yangtze River estuarine-inner shelf of the ECS (Fig. 1) were sampled using a stainless steel box corer on two occasions, first by the *R/V* Dong Fang Hong 2 research vessel of the Ocean University of China in 2006 and *R/V* Kan 407 research vessel in 2007.The samples were packed in aluminum foil and stored at -20 °C. Most of the surface samples were collected from the muddy areas of the estuary and inner shelf (Fig. 1).

2.2. Mercury analysis

The analytical procedure of Hg followed that described by Leipe et al. (2013). A DMA-80 Hg analyzer (Milestone Scientific Inc., USA) was used to measure Hg concentrations in sediments as it has a very low detection limit (Leipe et al., 2013). To ensure analytical accuracy and precision, standard reference materials (SRMs) were used, including environmental standards (ESS-4, 0.021 μg/g Hg) from the China Environmental Monitoring Station, and certified reference material (CRM) soil (GSS-13) from the Institute of Geophysical and Geochemical Exploration in China. The calibration curve included eight concentrations of Hg, from 0.004 to 20 ng. Standard materials were measured every 10 samples to control measurement quality and stability. For quality control, CRMs and sample replicates were included in the analytical procedure. The measured concentrations of SRMs were within their certified ranges and the recovery of Hg was 94.33 ± 9.53% (n=8).

2.3. Dataset consolidation and map generation

The total organic carbon (TOC), median diameter (MD), and ratio of carbon-to-nitrogen (C/N) datasets used in this study were from Hu et al. (2012), and the dataset of 16 polycyclic aromatic hydrocarbons (PAHs) cited in this study was from Lin et al. (2013). Detailed information on the original TOC, MD, and PAH datasets are summarized and abbreviated in Table S1. Contour maps were generated using isopleths based on the consolidation and standardization of these datasets using the Kriging gridding method in the surface mapping system (Surfer version 11.0, Golden Software, Inc).

2.4. Principal component analysis

Principal component analysis (PCA) is a multivariate analytical tool used to determine the sample distribution and study the relationships of measured parameters. Before the analysis, non-detectable values were replaced with concentration values equal to one-half the method detection limits. Then the raw data matrix was Z-score standardized and mid-range normalized to eliminate the influence of different units and ensure that each determined variable had equal weighting in the PCA. The PCA was performed using SPSS 13.0 for Windows (SPSS Inc., Chicago, IL, USA) (Hu et al., 2012). The Hg concentrations, individual compounds of 16 PAHs, MD, and TOC of the 70 sediment samples were used to perform the PCA analysis and SPSS was applied to extract the principal components (PCs) based on the correlation matrix. Principal components with eigenvalues >1 were considered to be factors for further examination.

3. Results and discussion

3.1. The concentration of Hg

The Hg concentration in the study area was 10–92 ng/g with a mean of 46 ± 17 ng/g, lower than those reported from the Northern Gulf of Mexico (10–200 ng/g) (Apeti et al., 2012), comparable to those from the Strait of Malacca, Malaysia (17–114 ng/g) (Zhuang and Gao., 2015), and higher than those in the Eastern Basin and Mediterranean Sea (<40 ng/g) (Ogrinc et al., 2007) (Table 1). A much higher concentration of Hg (150–1500 ng/g) was observed in the Kaohsiung River mouth, where Hg was emitted from municipal solid waste (Chen et al., 2012). These comparisons indicate that Hg concentrations in marine environments can vary by orders of magnitude (Ogrinc et al., 2007; Abi-Ghanem et al., 2011; Jin et al., 2012; Deng et al., 2013) (Table 1).

Mercury is persistent, bioaccumulated and toxic in the environment (Jiang et al., 2006; David et al., 2009; Neville et al., 2014; Chakraborty et al., 2015). Sediment quality guidelines, effects range low (ER-L), and effects range median (ER-M) were used to assess the potential biological risks of Hg (Table S2). Concentrations lower than the ER-L represent a minimal effect; those between the ER-L and ER-M represent a possible effect; and those above the ER-M represent a probable effect (Long et al., 1995). All of the Hg concentrations in the estuarine-inner shelf of the ECS were lower than the ER-L (Table S2), indicating that the Hg in sediment of the coastal ECS represented low-risk towards organisms.

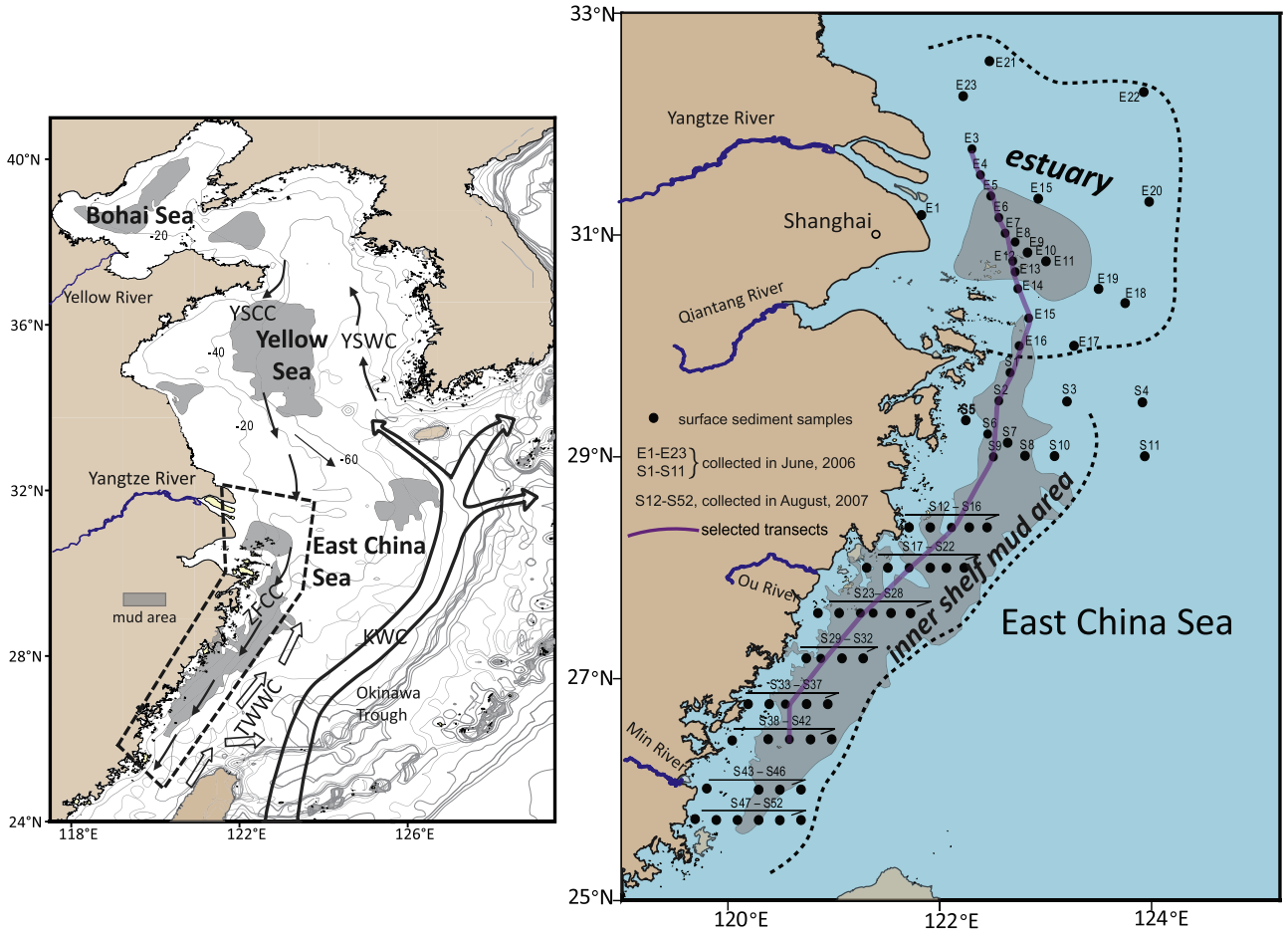

Fig. 1. Locations of sampling sites and circulation systems in the ECS (Circulation systems and mud areas are modified after Liu et al. (2007). KWC: Kuroshio Warm Current; TWWC: Taiwan Warm Current; ZFCC: Zhejiang-Fujian Coastal Current; YSCC: Yellow Sea Coastal Current; YSWC: Yellow Sea Warm Current).

3.2. Distribution of Hg and potential controlling factors

3.2.1. Spatial distribution of Hg and the influences of river input and hydrodynamic forces

The distributions of Hg, MD, TOC, and PAHs were shown in Fig. 2. The sediments in the inner shelf of the ECS was mainly composed of silt and clay with a median grain size of 4–7 Φ, while that of the YRE consisted largely of silt and clay with a median grain size of 3–7 Φ. The study area consisted mainly of fine-grained sediments. By ignoring the potential effect of sediment grain size, the average Hg concentration in the samples from muddy area of the YRE was 49 ± 13 ng/g, comparable to that in the muddy area of the Min-Zhe coast (52 ± 12 ng/g). In general, Hg concentration decreased with distance from the shore towards the outer shelf in the coastal ECS. The YRE had relatively higher Hg concentrations (> 50 ng/g), which extended along the muddy area of the inner shelf to the south, compared to those from outer sandy areas (Fig. 2a), suggesting that the occurrence of Hg in the coastal ECS directly depends on input from the Yangtze River. The spatial variability of Hg was similar to these land-based indicators in the coastal ECS, such as PAHs (Fig. 2a) (Lin et al., 2013) and perylene (Hu et al., 2014), indicating that the occurrence of Hg in the coastal ECS was primarily regulated by river input. In addition, Hg levels in sediment samples from the inner shelf (50 ± 14 ng/g) were higher than those in the YRE (37 ± 19 ng/g), consistent with the higher and less varied TOC and finer grain size in sediment samples from the southern inner shelf compared to the northern estuary (Hu et al., 2012). This observation indicates that hydrodynamic particle sorting could influence Hg concentration levels. This process could be ascribed to the re-

Table 1
Concentrations of Hg in sediments in the Yangtze River estuarine-inner shelf of the ECS and other estuarine/coastal areas in the world.

Locations	Hg concentrations (ng/g)	References
Estuarine-inner shelf, the East China Sea	10–92	This study
Inner shelf, the East China Sea	27–48	(Fang and Chen, 2010)
Middle shelf, the East China Sea	4–14	(Fang and Chen, 2010)
Eastern basin, the Mediterranean Sea	8–40	(Ogrinc et al., 2007)
Western basin, the Mediterranean Sea	78–90	(Ogrinc et al., 2007)
Strait of Malacca, Malaysia	17–114	(Zhuang and Gao, 2015)
Lebanese coast, Estern Mediterranean	100–650	(Abi-Ghanem et al., 2011)
Kaohsiung River mouth, Taiwan	150–1500	(Chen et al., 2012)
Northern Gulf of Mexico	10–200	(Apeti et al., 2012)
Continental coast of Shanghai	0–466	(Deng et al., 2013)
Jade Bay, Southern North Sea	8–243	(Jin et al., 2012)

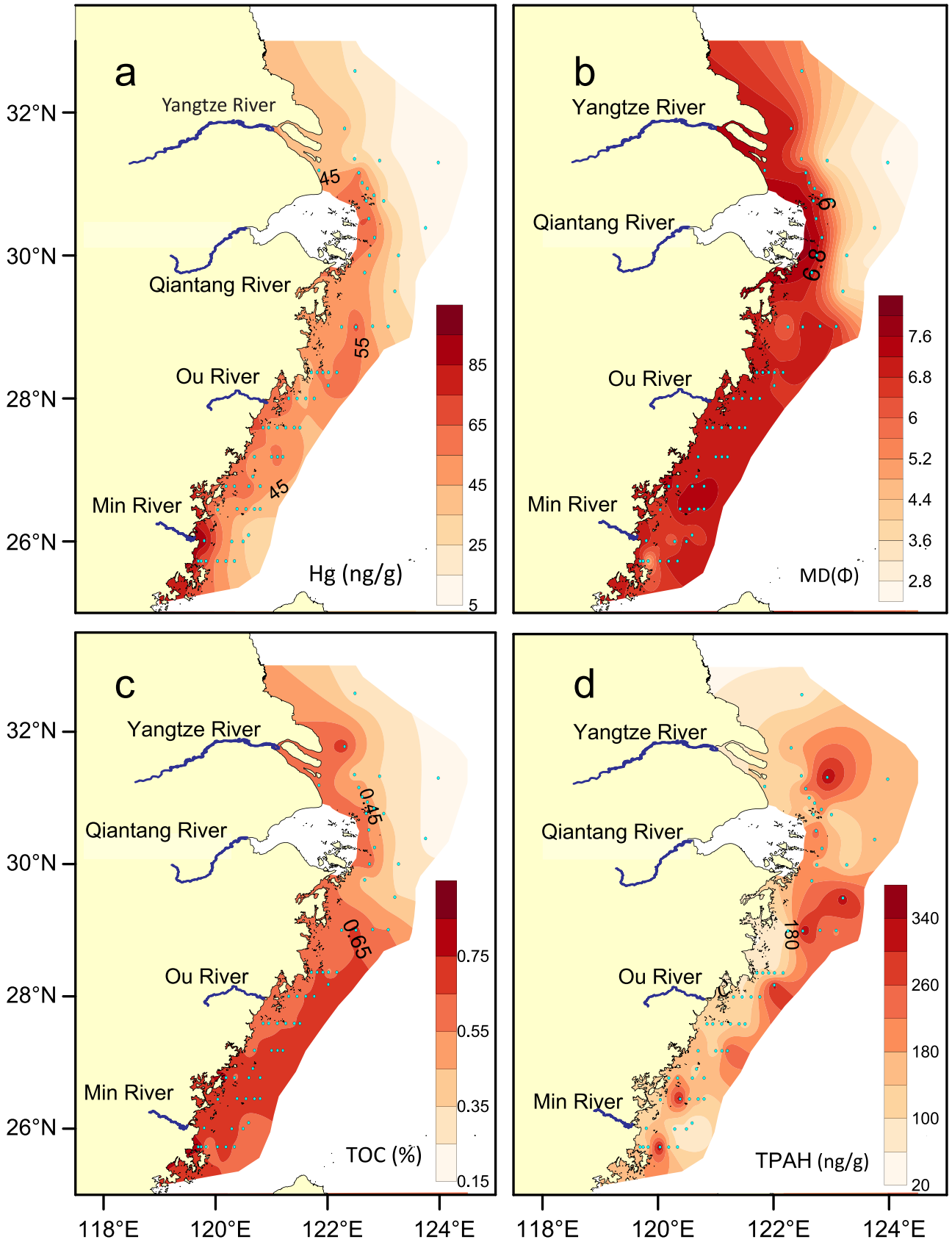

Fig. 2. Distribution of concentrations of Hg (a), MD (b), TOC (c), and PAHs (d) in sediments of the Yangtze estuarine-inner shelf in the ECS (Dataset sources: TOC and MD is from Hu et al. (2012) and PAHs are from Lin et al. (2013)).

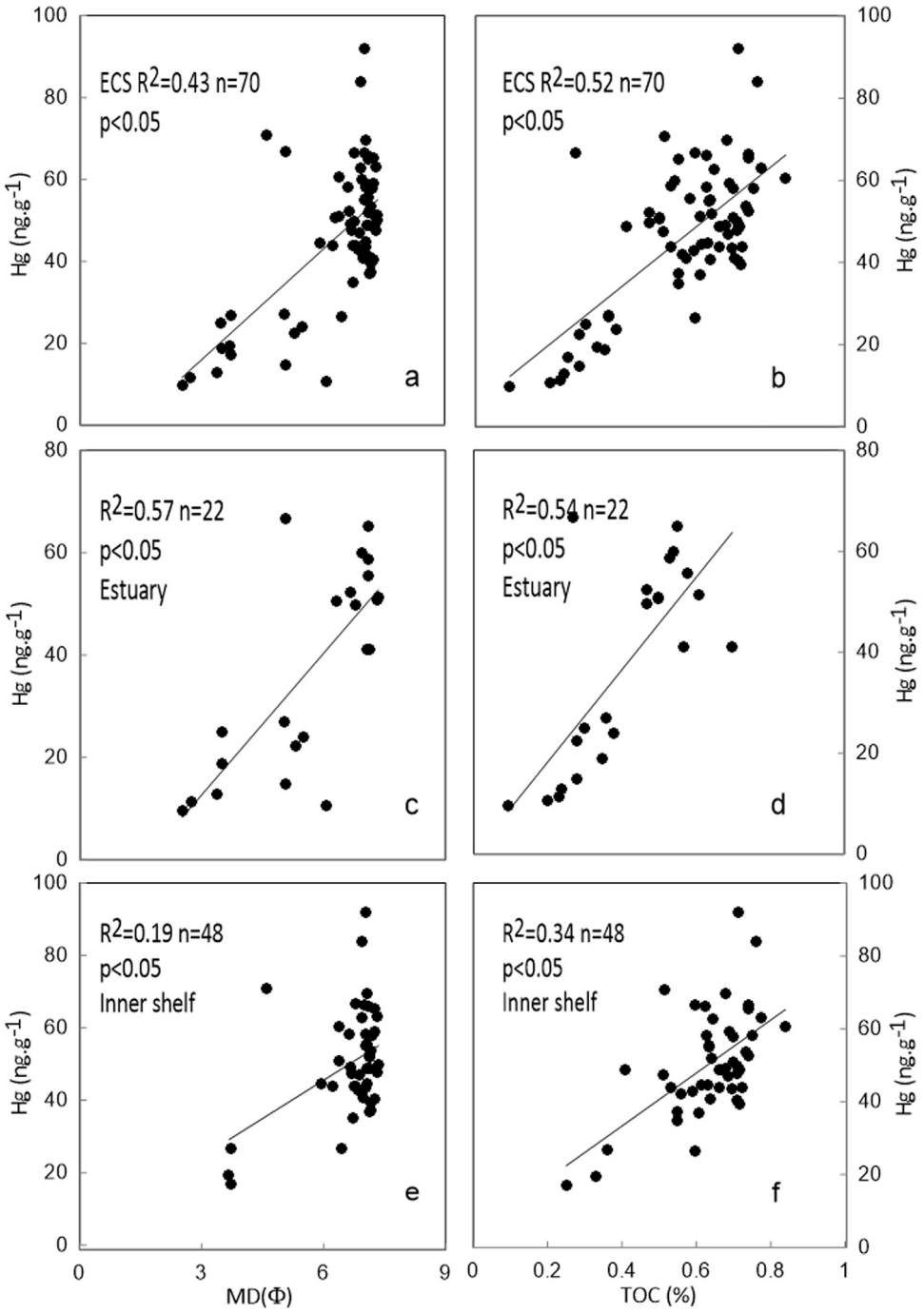

Fig. 3. Correlations of Hg with median diameters (a), (c) and (e), and TOC contents (b), (d) and (f) in sediments of the Yangtze estuary (Estuary) and inner shelf (inner shelf) of the ECS.

suspension and preferential dispersal of fine-grain sediments and associated materials southward along the inner shelf (Guo et al., 2003; Liu et al., 2006; Hu et al., 2012). Conversely, the low Hg levels in the YRE could be partially caused by a diluting effect due to the dominance of river input with a higher accumulation rate of sediments in this region compared to the southern inner shelf (Liu et al., 2006; Li et al., 2012; Lin et al., 2013).

In general, Hg was positively correlated with MD and TOC in the ECS (Fig. 3a and b), particularly for samples from the YRE (although this correlation could be partly driven by the mass of dataset at high MD) (Fig. 3c and d), suggesting that the sorption could influence the Hg enrichment in fine-grained sediments. Fine-grained sediments have a higher specific surface area of clay–silt particles than coarser sediments, which can increase the ability of trace and heavy metals to associate (Thorne and Nickless, 1981; Cauwet, 1987; Araujo et al., 1988). In the southern inner shelf, there was a poor correlation between MD and Hg, probably because of the small variation in grain size and Hg abundance (Fig. 3e).

3.2.2. Potential effect of sedimentary organic matter on the distribution of Hg

Mercury is usually correlated with TOC in estuarine, coastal, and open sea sediments (Yin et al., 2013; Sanei et al., 2014). However, in this study, the relationship between Hg and TOC varied and was only significant in the estuarine area (Fig. 3d, R^2=0.54, n=22). This could be due to their similar direct fluvial input pathways and/or the overall hydrodynamics. Moreover, as noted above, the relatively poor correlations between TOC, MD, and Hg in the samples from the inner shelf

(Fig. 3f) suggested an insignificant influence of grain size on the relationship between Hg and TOC in this region. It was reported that the nature of OM in sediments could influence the distribution and speciation of Hg by providing strong binding sites in sediment surface (Mason and Lawrence, 1999; Hammerschmidt and Fitzgerald, 2004; Hammerschmidt et al., 2004; Stoichev et al., 2004). Actually, the association between OM and Hg in sediment has also been extensively studied before (Gagnon et al., 1997; Stoichev; et al., 2004; Sanei and Goodarzi, 2006; Stern et al., 2009; Sanei et al., 2014; Chakraborty et al., 2015); and it was found that various types of OM play different role in the distribution and accumulation of Hg in sediment, *i.e.* as compared to the allochthonous refractory OM *e.g.,,* woody material and reworked OM), the autochthonous labile OM (algal-derived lipids and various pigments) may provide a substrate with enormous surface area by concentrating on the finer sediment size fractions, which led to a strong affinity between Hg and the algal materials (Regnell et al., 1997; Sanei and Goodarzi, 2006). Recently, it was also found that the TOC (influenced by marine OM) probably having better Hg complexing capacity due to the available sufficient Hg-binding sites within this autochthonous labile organic components (Chakraborty et al., 2015). In the coastal ECS, as reflected by the alongshore transect of bulk OM indices, such as C/N (Fig. 4), the contribution of terrestrial OM was significant in the north; while more marine-derived OM was present at the southern inner shelf (Hu et al., 2012). The alongshore north–south shift in the composition of the sedimentary organic matter (SOM) pool could affect the geochemical behavior of Hg in the region. To diminish the greatest effect of grain size, an alongshore transect was selected from the north to the south, focusing only on fine-grained sediment samples (Fig. 1). The alongshore C/N and Hg/TOC ratios in this transect were inversely correlated to some extent (Fig. 4); especially in the south, a lower C/N ratio was coupled with a relatively higher Hg/TOC ratio. This preliminary result thus may indicate that as compared to the more refractory terrestrial sedimentary OM in the northern estuary, the TOC in the sediments from the southern inner shelf with more fraction of marine-derived autochthonous OM probably provide higher Hg-binding capacity (Chakraborty et al., 2015), which could potentially enhance its property as a sink for Hg in the coastal ECS.

3.3. Principal component analysis (PCA) with implication for the input pathway of Hg

After performing PCA on the datasets, including PAHs, Hg, TOC, and sediment grain size (Table S1), the scree plot of eigenvalues indicated that 94% of the data variance could be explained by the first three PCs. The first two PCs (PC1 and PC2) explained 85% of the total

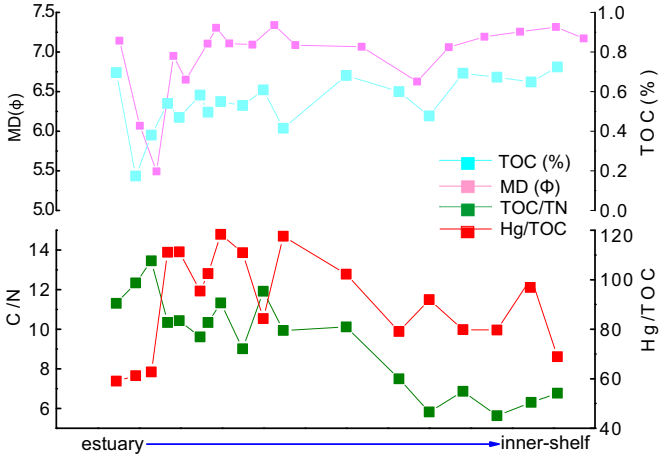

Fig. 4. Distribution of TOC, median diameters, values of C/N, Hg/TOC concentrations of the selected alongshore transect from the estuarine mud to the inner shelf region of the ECS.

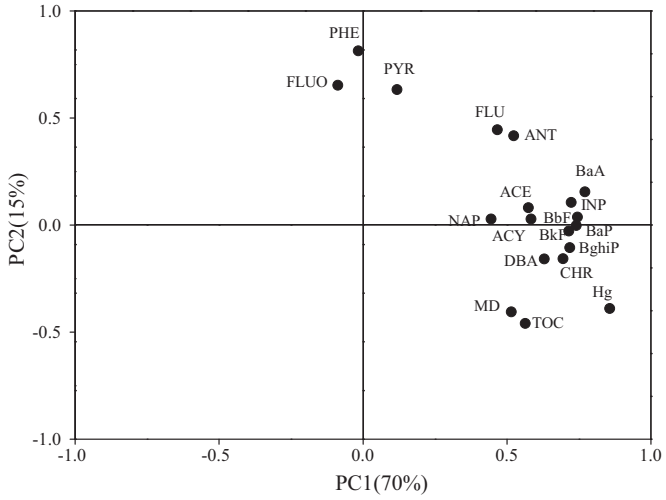

Fig. 5. Plot of loadings of PC1 and PC2 from PCA for the datasets of Hg, TOC, MD and individual PAH compounds of the surface sediment samples in the ECS.

data variance (Fig. 5); while PC3 explained < 10% of the variance, which was poorly correlated with these individual variables. PC1, accounting for 70% of the data variance, was distinguished by high positive loadings of TOC, high-molecular-weight (HMW) PAHs, Hg, and MD. PC2 explained 15% of the total data variance, characterized by the positive loading of low-molecular-weight PAHs and negative loading of MD, TOC, and Hg. Mercury and PAHs usually have common sources and pathways into the environment (Parsons et al., 2014). For instance, there was a strong correlation between total PAHs and Hg in lakes in Michigan, USA (Parsons et al., 2014). However, in this study, there was only a moderate correlation between Hg and 5-ring and 6-ring PAHs (Fig. 6a, R^2=0.41, $p < 0.05$) in the YRE and a poor correlation in the southern inner shelf (Fig. 6b, R^2=0.13, $p < 0.05$). Considering the dominant fluvial input of land-based components in the coastal ECS, PC1 mainly revealed the common input pathway of Hg and the HMW PAHs as part of terrigenous SOM input from river discharge, particularly in the samples from the YRE. The high positive loading of fine-grained sediments on PC1 and its correlation with Hg in the YRE support the effect of hydrodynamic forces on the behavior of Hg in estuarine mud areas. The muddy area in the coastal ECS was reported to be the main sink for terrigenous SOM from the Yangtze River (Liu et al., 2006; Hu et al., 2012). Therefore, the covariance of Hg and HMW PAHs could be partially due to the same direct land-based fluvial input and their coupled sedimentary dynamics.

The correlation between Hg and HMW PAHs was poor in the southern inner shelf (Fig. 6b), suggesting a decoupling of either the behavior or sources of Hg and HMW PAHs therein. As noted above, the alongshore shift of the composition of SOM could exert a geochemical effect on sedimentary Hg in this area; while the HMW PAHs and SOM in the southern inner shelf have not reached equilibrium (Lin et al., 2013). Furthermore, different sources of Hg and PAHs could also partially explain their decoupling in the coastal ECS, in spite of the overall combustion-derived processes as reflected by their grouping in the PCA (Fig. 5). Mercury mainly originates from coal combustion and various industrial sources, such as non-ferrous smelting (Jiang et al., 2006); while high-temperature pyrogenic processes generate 4–6-ring PAHs, mainly from incomplete fossil fuel combustion and biomass burning (Soclo et al., 2000; Mai et al., 2003). Jiang et al. (2006) reported that a total of ~1400–2700 t Hg has been released from the chlor–alkali industry in China since the 1950s.

3.4. Deposition flux of Hg

The mass inventory of Hg in the study area was estimated according

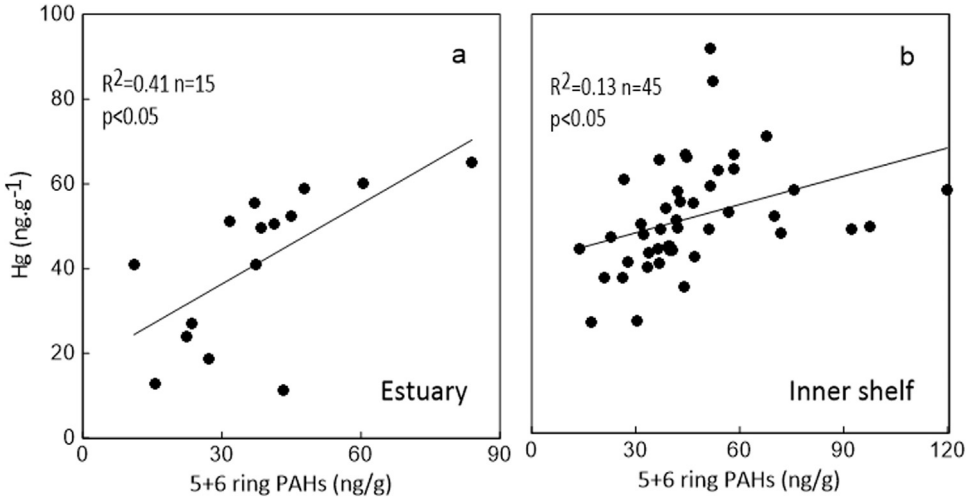

Fig. 6. Correlations of Hg with 5+6 ring PAHs in the sediments of the Yangtze estuarine (Estuary) and inner shelf (Inner shelf) of the ECS.

to Di Francesco et al. (1998) and Wang et al. (2006). The study area in this work was divided into 70 homogeneous sectors, with sampling sites located in the center of their respective sectors. The mass inventory of Hg in sediment was calculated according to the following equation:

$$I = \sum_{i=1}^{70} Ci \cdot Ai \cdot d \cdot pi$$

where Ci is the Hg concentration in the sediment sample; Ai is the water surface area (Table S3); d is the recommended sediment dry density of 1.2 g/cm^3 for this area according to Liu et al. (2007); and pi is sedimentary rate for each sample site based on Demaster et al. (1985), Huh and Su (1999), and Liu et al. (2006, 2007).

Relatively high Hg deposition fluxes (5.8–120 ng/cm^2 y) were observed along the inner shelf due to higher concentrations of Hg and mass accumulation rates (MAR) than those in the estuary (Fig. 7). Fang and Chen (2010) estimated that the Hg deposition flux in the ECS was about 0.4–49 ng/cm^2 y, lower than that observed in this study, which could be attributed to the varying Hg concentrations and MAR in this area. The sediment samples of former study were mainly from the middle and outer shelf in the ECS in contrast to those on the inner shelf mud area with a higher MAR (Huh et al., 1999). Furthermore, the higher Hg concentrations in this study were probably influenced by recent Hg accumulation (2006–2007) compared to the samples of previous study collected in late 1990s. In the comparison of worldwide aquatic environments (Table 2), Hg deposition flux in the Lake Tahoe, California-Nevada was as low as 1.5–2 ng/cm^2 y (Drevnick et al., 2010), and with a moderate range of 76–116 ng/cm^2 y in the Deep Bay, China (Li et al., 2016); while the high Hg flux was observed in the Guanabara Bay (100–1800 ng/cm^2 y) (Covelli et al., 2012).

Our sampling sites covered an area of ~100,000 km^2, extending ~1000 km from the mouth of the Yangtze River to the Min River in the muddy area of the inner shelf (Lin et al., 2013). The total mass inventory of Hg for the studied region was estimated to be ~51 t/y, with an average deposition flux of 62 ± 34 ng/cm^2 y. The mass of particulate Hg from riverine discharge to ocean margins, such as the Arctic Ocean and the Mediterranean Sea, is about 15 ± 12 t/y and 14. ± 10 t/y, respectively, and in the North Atlantic and Indian Oceans, it is about 32 ± 26 t/y and 502 ± 502 t/y, respectively (Amos et al., 2014). Liu et al. (2016) reported that the concentration of Hg in the Yangtze River gradually increased from the 1980 s to the 2000 s due to the recent input of the Yangtze River. It was estimated that a total of 240 ± 23 t Hg was exported in 2012 from mainland China into the sea (Liu et al., 2016). For the various sources of Hg-rivers, i.e., industrial wastewater, domestic sewage, groundwater, non-point sources, and

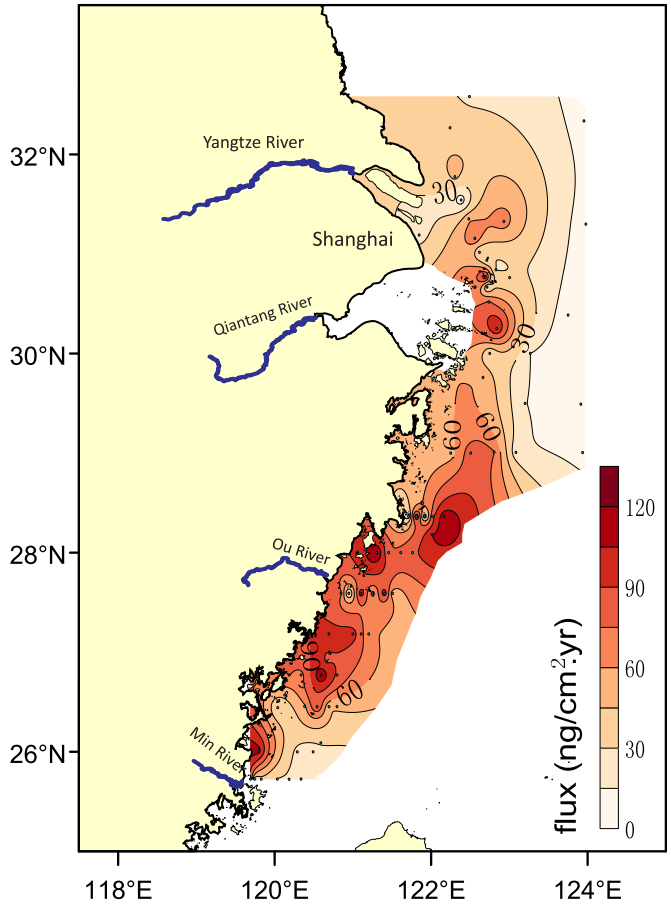

Fig. 7. Deposition flux of Hg in the estuarine-inner shelf of the ECS.

coastal erosion, the Hg from rivers amounts to 160 ± 21 t/y and plays a leading role in the global balance of Hg (Liu et al., 2016). These above results indicated that the deposition flux of Hg in the estuarine-inner shelf of the ECS occupied one-fifth of total Hg from mainland China into the sea, and more importantly, it was about one-third for the Chinese riverine discharged-Hg into the sea, the study area thus serve as a major sink of Hg in the marginal seas off China. Amos et al. (2014) estimated that one-third of post-1850 anthropogenic Hg release was sequestered in ocean margin sediments, and reported that global present-day Hg discharges from rivers to ocean margins were 5500 ± 2700 t/y, of which 28% reaches the open ocean and the rest was

Table 2
Comparison of the deposition flux of Hg in the ECS and worldwide marine environments.

Locations	Deposition Flux (ng/cm^2 yr)	References
Estuarine-inner shelf in the ECS	6–120	This study
Inner shelf, the East China Sea	4–49	(Fang and Chen., 2010)
Middle shelf, the East China Sea	0–9	(Fang and Chen., 2010)
Eastern basin, the Mediterranean Sea	0.09–0.18	(Ogrinc et al., 2007)
Western basin, the Mediterranean Sea	0.38–1.13	(Ogrinc et al., 2007)
the Guanabara Bay	100–1800	(Covelli et al., 2012)
Avicennia marinaforest of Deep Bay, China	76–116 (cores)	(Li et al., 2016)
Lake Tahoe, California-Nevada	1.5–2	(Drevnick et al., 2010)

deposited to ocean margin sediments. These estimated results supports that the estuarine-inner shelf of the ECS could play a significant role in the Hg biogeochemical cycle on a global scale considering that there is only 100,000 km^2 for the study area.

Acknowledgments

This work was supported by the National Natural Science Foundation of China (Nos. 41376051 and U1606401), the National Key Research Program of China (2016YFA0601903), the National Programme on Global Change and Air-Sea Interaction (GASI-GEOGE-03), and in part by the China Postdoctoral Science Foundation (No. 2012T50596). We thank the Coastal Investigation and Research Project of China (908-ZC-I-05) for providing the background information of the samples. We also wish to thank the crews of the *R/V Dong Fang Hong 2* and of the *Kan 407* for collecting the sediment samples. We thank the anonymous reviewers for their constructive comments that greatly improved this work.

Appendix A. Supplementary material

Supplementary data associated with this article can be found in the online version at http://dx.doi.org/10.1016/j.csr.2016.11.004.

References

Abi-Ghanem, C., Nakhlé, K., Khalaf, G., Cossa, D., 2011. Mercury distribution and methylmercury mobility in the sediments of three sites on the Lebanese Coast, Eastern Mediterranean. Arch. Environ. Contam. Toxicol. 60, 394–405.
Amos, H.M., Jacob, D.J., Kocman, D., Horowitz, H.M., Zhang, Y.X., Dutkiewicz, S., Horvat, M., Corbitt, E.S., Krabbenhoft, D.P., Sunderland, E.M., 2014. Global biogeochemical implications of mercury discharges from rivers and sediment burial. Environ. Sci. Technol. 48, 9514–9522.
Apeti, D.A., Lauenstein, G.G., Evans, D.W., 2012. Recent status of total mercury and methylmercury in the coastal waters of the northern Gulf of Mexico using oysters and sediments from NOAA's mussel watch program. Mar. Pollut. Bull. 64, 2399–2408.
Araujo, M.F.D., Bernard, P.C., Vangrieken, R.E., 1988. Heavy-metal contamination in sediments from the Belgian coast and Scheldt estuary. Mar. Pollut. Bull. 19, 269–273.
Bianchi, T.S., Allison, M.A., 2009. Large-river delta-front estuaries as natural "recorders" of global environmental change. Proc. Natl. Acad. Sci. USA 106, 8085–8092.
Cauwet, G., 1987. Influence of sedimentological features on the distribution of trace-metals in marine-sediments. Mar. Chem. 22, 221–234.
Chakraborty, P., Babu, P.V.R., Acharyya, T., Bandyopadhyay, D., 2010. Stress and toxicity of biologically important transition metals (Co, Ni, Cu and Zn) on phytoplankton in a tropical freshwater system: an investigation with pigment analysis by HPLC. Chemosphere 80, 548–553.
Chakraborty, P., Sarkar, A., Vudamala, K., Naik, R., Nath, B.N., 2015. Organic matter – a key factor in controlling mercury distribution in estuarine sediment. Mar. Chem. 173, 302–309.
Chen, B., Fan, D., Li, W., Wang, L., Zhang, X., Liu, M., Guo, Z., 2014. Enrichment of heavy metals in the inner shelf mud of the East China Sea and its indication to human activity. Cont. Shelf Res. 90, 163–169.
Chen, C.W., Chen, C.F., Dong, C.D., 2012. Contamination and potential ecological risk of mercury in sediments of Kaohsiung River mouth, Taiwan. Int. J. Environ. Sci. Dev. 3, 66–71.
Covelli, S., Protopsalti, I., Acquavita, A., Sperle, M., Bonardi, M., Emili, A., 2012. Spatial variation, speciation and sedimentary records of mercury in the Guanabara Bay (Rio de Janeiro, Brazil). Cont. Shelf Res. 35, 29–42.
David, N., McKee, L.J., Black, F.J., Flegal, A.R., Conaway, C.H., Schoellhamer, D.H., Ganju, N.K., 2009. Mercury concentrations and loads in a large river system tributary to San Francisco Bay California, USA. Environ. Toxicol. Chem. 28, 2091–2100.
Demaster, D.J., McKee, B.A., Nittrouer, C.A., Qian, J.C., Cheng, G.D., 1985. Rates of sediment accumulation and particle reworking based on radiochemical measurements from continental-shelf deposits in the East China Sea. Cont. Shelf Res. 4, 143–158.
Deng, H., Wang, D., Chen, Z., Xu, S., Zhang, J., Delaune, R.D., 2013. A comprehensive investigation and assessment of mercury in intertidal sediment in continental coast of Shanghai. Environ. Sci. Pollut. Res. 20, 6297–6305.
Di Francesco, F., Ferrara, R., Mazzolai, B., 1998. Two ways of using a chamber for mercury flux measurement – a simple mathematical approach. Sci. Total Environ. 213, 33–41.
Drevnick, P.E., Shinneman, A.L.C., Lamborg, C.H., Engstrom, D.R., Bothner, M.H., Oris, J.T., 2010. Mercury flux to sediments of Lake Tahoe, California-Nevada. Water Air Soil Pollut. 210, 399–407.
Elbaz-Poulichet, F., Dezileau, L., Freydier, R., Cossa, D., Sabatier, P., 2011. A 3500-year record of Hg and Pb contamination in a mediterranean sedimentary archive (the Pierre Blanche Lagoon, France). Environ. Sci. Technol. 45, 8642–8647.
Ernst, W.G., 2012. Overview of naturally occurring Earth materials and human health concerns. J. Asian Earth Sci. 59, 108–126.
Fang, T.H., Chen, R.Y., 2010. Mercury contamination and accumulation in sediments of the East China Sea. J. Environ. Sci. 22, 1164–1170.
Frignani, M., Bellucci, L.G., Favotto, M., Albertazzi, S., 2005. Pollution historical trends as recorded by sediments at selected sites of the Venice Lagoon. Environ. Int. 31, 1011–1022.
Gagnon, C., Pelletier, É., Mucci, A., 1997. Behaviour of anthropogenic mercury in coastal marine sediments. Mar. Chem. 59, 159–176.
Guo, Z.G., Sheng, L.F., Feng, J.L., Fang, M., 2003. Seasonal variation of solvent extractable organic compounds in the aerosols in Qingdao, China. Atmos. Environ. 37, 1825–1834.
Gustin, M.S., Lindberg, S.E., Weisberg, P.J., 2008. An update on the natural sources and sinks of atmospheric mercury. Appl. Geochem. 23, 482–493.
Hammerschmidt, C.R., Fitzgerald, W.F., 2004. Geochemical controls on the production and distribution of methylmercury in near-shore marine sediments. Environ. Sci. Technol. 38, 1487–1495.
Hammerschmidt, C.R., Fitzgerald, W.F., Lamborg, C.H., Balcom, P.H., Visscher, P.T., 2004. Biogeochemistry of methylmercury in sediments of Long Island Sound. Mar. Chem. 90, 31–52.
Holmes, C.D., Jacob, D.J., Yang, X., 2006. Global lifetime of elemental mercury against oxidation by atomic bromine in the free troposphere. Geophys. Res. Lett. 33, L20808 .
Hu, L.M., Shi, X.F., Lin, T., Guo, Z.G., Ma, D.Y., Yang, Z.S., 2014. Perylene in surface sediments from the estuarine-inner shelf of the East China Sea: a potential indicator to assess the sediment footprint of large river influence. Cont. Shelf Res. 90, 142–150.
Hu, L.M., Shi, X.F., Yu, Z.G., Lin, T., Wang, H.J., Ma, D.Y., Guo, Z.G., Yang, Z.S., 2012. Distribution of sedimentary organic matter in estuarine–inner shelf regions of the East China Sea: implications for hydrodynamic forces and anthropogenic impact. Mar. Chem. 142–144, 29–40.
Huh, C.A., Su, C.C., 1999. Sedimentation dynamics in the East China Sea elucidated from Pb-210, Cs-137 and Pu-239, Pu-240. Mar. Geol. 160, 183–196.
Hylander, L.D., Goodsite, M.E., 2006. Environmental costs of mercury pollution. Sci. Total Environ. 368, 352–370.
Jiang, G.B., Shi, J.B., Feng, X.B., 2006. Mercury pollution in China. Environ. Sci. Technol. 40, 3672–3678.
Jin, H., Liebezeit, G., Ziehe, D., 2012. Distribution of total mercury in surface sediments of the Western Jade Bay, Lower Saxonian Wadden Sea, Southern North Sea. Bull. Environ. Contam. Toxicol. 88, 597–604.
Jonsson, S., Skyllberg, U., Nilsson, M.B., Westlund, P.O., Shchukarev, A., Lundberg, E., Bjorn, E., 2012. Mercury methylation rates for geochemically relevant Hg-II species in sediments. Environ. Sci. Technol. 46, 11653–11659.
Keeler, G.J., Landis, M.S., Norris, G.A., Christianson, E.M., Dvonch, J.T., 2006. Sources of mercury wet deposition in Eastern Ohio, USA. Environ. Sci. Technol. 40, 5874–5881.
Leipe, T., Moros, M., Kotilainen, A., Vallius, H., Kabel, K., Endler, M., Kowalski, N., 2013. Mercury in Baltic Sea sediments-Natural background and anthropogenic impact. Chem. ErdeGeochem. 73, 249–259.
Li, C., Yang, S.Y., Lian, E.G., Bi, L., Zhang, Z.F., 2015. A review of comminution age method and its potential application in the East China Sea to constrain the time scale of sediment source-to-sink process. J. Ocean Univ. China 14, 399–406.

Li, P., Feng, X.B., Shang, L.H., Qiu, G.L., Meng, B., Zhang, H., Guo, Y.N., Liang, P., 2011. Human co-exposure to mercury vapor and methylmercury in artisanal mercury mining areas, Guizhou, China. Ecotoxicol. Environ. Saf. 74, 473–479.
Li, R.L., Chai, M.W., Guo, M.X., Qiu, G.Y., 2016. Sediment accumulation and mercury (Hg) flux in Avicennia marina forest of Deep Bay, China. Estuar. Coast. Shelf Sci. 177, 41–46.
Li, Y.Y., Lin, T., Chen, Y., Hu, L.M., Guo, Z.G., Zhang, G., 2012. Polybrominated diphenyl ethers (PBDEs) in sediments of the coastal East China Sea: occurrence, distribution and mass inventory. Environ. Pollut. 171, 155–161.
Lin, T., Hu, L.M., Guo, Z.G., Zhang, G., Yang, Z.S., 2013. Deposition fluxes and fate of polycyclic aromatic hydrocarbons in the Yangtze River estuarine-inner shelf in the East China Sea. Glob. Biogeochem. Cycles 27, 77–87.
Lindberg, S., Bullock, R., Ebinghaus, R., Engstrom, D., Feng, X.B., Fitzgerald, W., Pirrone, N., Prestbo, E., Seigneur, C., 2007. A synthesis of progress and uncertainties in attributing the sources of mercury in deposition. Ambio 36, 19–32.
Liu, J.P., Li, A.C., Xu, K.H., Velozzi, D.M., Yang, Z.S., Milliman, J.D., DeMaster, D.J., 2006. Sedimentary features of the Yangtze River-derived along-shelf clinoform deposit in the East China Sea. Cont. Shelf Res. 26, 2141–2156.
Liu, J.P., Xu, K.H., Li, A.C., Milliman, J.D., Velozzi, D.M., Xiao, S.B., Yang, Z.S., 2007. Flux and fate of Yangtze River sediment delivered to the East China Sea. Geomorphology 85, 208–224.
Liu, M.D., Chen, L., Wang, X.W., Zhang, W., Tong, Y.D., Ou, L.B., Xie, H., Shen, H.Z., Ye, X.J., Deng, C.Y., Wang, H.H., 2016. mercury export from mainland China to adjacent seas and ItsInfluence on the marine mercury balance. Environ. Sci. Technol. 50, 6224–6232.
Long, E.R., Macdonald, D.D., Smith, S.L., Calder, F.D., 1995. Incidence of adverse biological effects within ranges of chemical concentrations in marine and estuarine sediments. Environ. Manag. 19, 81–97.
Luo, W., Lu, Y.L., Wang, T.Y., Hu, W.Y., Jiao, W.T., Naile, J.E., Khim, J.S., Giesy, J.P., 2010. Ecological risk assessment of arsenic and metals in sediments of coastal areas of northern Bohai and Yellow Seas, China. Ambio 39, 367–375.
Mai, B.X., Qi, S.H., Zeng, E.Y., Yang, Q.S., Zhang, G., Fu, J.M., Sheng, G.Y., Peng, P.N., Wang, Z.S., 2003. Distribution of polycyclic aromatic hydrocarbons in the coastal region off Macao, China: Assessment of input sources and transport pathways using compositional analysis. Environ. Sci. Technol. 37, 4855–4863.
Mason, R.P., Lawrence, A.L., 1999. Concentration, distribution, and bioavailability of mercury and methylmercury in sediments of Baltimore Harbor and Chesapeake Bay, Maryland, USA. Environ. Toxicol. Chem. 18, 2438–2447.
Meng, M., Shi, J.B., Yun, Z.J., Zhao, Z.S., Li, H.J., Gu, Y.X., Shao, J.J., Chen, B.W., Li, X.D., Jiang, G.B., 2014. Distribution of mercury in coastal marine sediments of China: sources and transport. Mar. Pollut. Bull. 88, 347–353.
Milliman, J.D., Beardsley, R.C., Yang, Z.S., Limeburner, R., 1985. Modern Huanghe-derived muds on the outer shelf of the East China Sea-Indentification and potential transport mechanisms. Cont. Shelf Res. 4, 175–188.
Moreno, M.J., Perrot, V., Epov, V.N., Monperrus, M., Amouroux, D., 2013. Chemical kinetic isotope fractionation of mercury during abiotic methylation of Hg(II) by methylcobalamin in aqueous chloride media. Chem. Geol. 336, 26–36.
Neville, L.A., Patterson, R.T., Gammon, P., Macumber, A.L., 2014. Relationship between ecological indicators (Arcellacea), total mercury concentrations and grain size in lakes within the Athabasca oil sands region, Alberta. Environ. Earth Sci. 72, 577–588.
Ogrinc, N., Monperrus, M., Kotnik, J., Fajon, V., Vidimova, K., Amouroux, D., Kocman, D., Tessier, E., Zizek, S., Horvat, M., 2007. Distribution of mercury and methylmercury in deep-sea surficial sediments of the Mediterranean sea. Mar. Chem. 107, 31–48.
Parsons, M.J., Long, D.T., Giesy, J.P., Kannan, K., 2014. Inferring sources for mercury to inland lakes using sediment chronologies of polycyclic aromatic hydrocarbons. Environ. Sci. Process. Impacts 16, 2108–2116.
Pena-Fernandez, A., Gonzalez-Munoz, M.J., Lobo-Bedmar, M.C., 2014. Establishing the importance of human health risk assessment for metals and metalloids in urban environments. Environ. Int. 72, 176–185.
Peng, J.F., Song, Y.H., Yuan, P., Cui, X.Y., Qiu, G.L., 2009. The remediation of heavy metals contaminated sediment. J. Hazard. Mater. 161, 633–640.
Regnell, O., Ewald, G., Lord, E., 1997. Factors controlling temporal variation in methyl mercury levels in sediment and water in a seasonally stratified lake. Limnol. Oceanogr. 42, 1784–1795.
Sanei, H., Goodarzi, F., 2006. Relationship between organic matter and mercury in recent lake sediment: the physical–geochemical aspects. Appl. Geochem. 21, 1900–1912.
Sanei, H., Outridge, P.M., Stern, G.A., Macdonald, R.W., 2014. Classification of mercury-labile organic matter relationships in lake sediments. Chem. Geol. 373, 87–92.
Schroeder, W.H., Munthe, J., 1998. Atmospheric mercury – an overview. Atmos. Environ. 32, 809–822.
Soclo, H.H., Garrigues, P., Ewald, M., 2000. Origin of polycyclic aromatic hydrocarbons (PAHs) in coastal marine sediments: case studies in Cotonou (Benin) and Aquitaine (France) areas. Mar. Pollut. Bull. 40, 387–396.
Stein, E.D., Cohen, Y., Winer, A.M., 1996. Environmental distribution and transformation of mercury compounds. Crit. Rev. Environ. Sci. Technol. 26, 1–43.
Stern, G., Sanei, H., Roach, P., Delaronde, J., Outridge, P., 2009. Historical interrelated variations of mercury and aquatic organic matter in lake sediment cores from a subarctic lake in Yukon, Canada: further evidence toward the algal-mercury scavenging hypothesis. Environ. Sci. Technol. 43, 7684–7690.
Stoichev, T., Amouroux, D., Wasserman, J.C., Point, D., De Diego, A., Bareille, G., Donard, O.F.X., 2004. Dynamics of mercury species in surface sediments of a macrotidal estuarine-coastal system (Adour River, Bay of Biscay). Estuar. Coast. Shelf Sci. 59, 511–521.
Streets, D.G., Hao, J.M., Wu, Y., Jiang, J.K., Chan, M., Tian, H.Z., Feng, X.B., 2005. Anthropogenic mercury emissions in China. Atmos. Environ. 39, 7789–7806.
Thorne, L.T., Nickless, G., 1981. The relation between heavy-metals and partical-size fractions within the severn estuary (UK) inter-tidal sediments. Sci. Total Environ. 19, 207–213.
Ullrich, S.M., Tanton, T.W., Abdrashitova, S.A., 2001. Mercury in the aquatic environment: a review of factors affecting methylation. Crit. Rev. Environ. Sci. Technol. 31, 241–293.
Wang, D., He, L., Shi, X., Wei, S., Feng, X., 2006. Release flux of mercury from different environmental surfaces in Chongqing, China. Chemosphere 64, 1845–1854.
Wang, H.T., Wang, J.W., Liu, R.M., Yu, W.W., Shen, Z.Y., 2015. Spatial variation, environmental risk and biological hazard assessment of heavy metals in surface sediments of the Yangtze River estuary. Mar. Pollut. Bull. 93, 250–258.
Wang, J.W., Liu, R.M., Zhang, P.P., Yu, W.W., Shen, Z.Y., Feng, C.H., 2014. Spatial variation, environmental assessment and source identification of heavy metals in sediments of the Yangtze River Estuary. Mar. Pollut. Bull. 87, 364–373.
Yan, C.Z., Li, Q.Z., Zhang, X., Li, G.X., 2010. Mobility and ecological risk assessment of heavy metals in surface sediments of Xiamen Bay and its adjacent areas, China. Environ. Earth Sci. 60, 1469–1479.
Yang, Z., Wang, H., Saito, Y., Milliman, J.D., Xu, K., Qiao, S., Shi, G., 2006. Dam impacts on the Changjiang (Yangtze) River sediment discharge to the sea: the past 55 years and after the three Gorges Dam. Water Resour. Res. 42, W04407.
Yin, Y.G., Li, Y.B., Ma, X., Liu, J.F., Jiang, G.B., 2013. Role of natural organic matter in the biogeochemical cycle of mercury: binding and molecular transformation. Prog. Chem. 25, 2169–2177.
Zhang, T., Kucharzyk, K.H., Kim, B., Deshusses, M.A., Hsu-Kim, H., 2014. Net methylation of mercury in estuarine sediment microcosms amended with dissolved, nanoparticulate, and microparticulate mercuric sulfides. Environ. Sci. Technol. 48, 9133–9141.
Zhou, F., Guo, H.C., Hao, Z.J., 2007. Spatial distribution of heavy metals in Hong Kong's marine sediments and their human impacts: a GIS-based chemometric approach. Mar. Pollut. Bull. 54, 1372–1384.
Zhuang, W., Gao, X.L., 2015. Distributions, sources and ecological risk assessment of arsenic and mercury in the surface sediments of the southwestern coastal Laizhou Bay, Bohai Sea. Mar. Pollut. Bull. 99, 320–327.